

## Three relaxation processes from an electric-field-induced polar structure in a columnar liquid crystalline urea derivative

Yoshinori Okada,<sup>1</sup> Shohei Matsumoto,<sup>1</sup> Fumito Araoka,<sup>1</sup> Masanao Goto,<sup>1</sup> Yoichi Takanishi,<sup>1</sup> Ken Ishikawa,<sup>1</sup> Shoichiro Nakahara,<sup>2</sup> Keiki Kishikawa,<sup>2</sup> and Hideo Takezoe<sup>1</sup>

<sup>1</sup>*Department of Organic and Polymeric Materials, Tokyo Institute of Technology, O-okayama, Meguro-ku, Tokyo 152-8552, Japan*

<sup>2</sup>*Department of Applied Chemistry and Biotechnology, Chiba University, 1-33 Yayoi-cho, Inage-ku, Chiba 263-8522, Japan*

(Received 28 March 2007; published 2 October 2007)

We have studied the polarization relaxation process after removing an applied electric field in the columnar hexagonal phase of *N,N'*-bis(3,4,5-trihexadecyloxyphenyl)urea by means of second-harmonic generation (SHG), switching current, and texture observation. Transient SHG and current associated by sudden field change show polarization switching associated with a molecular reorientation of about a few ms depending on the field strength. Furthermore, the texture observation reveals a column undulation process during 10 s to 1 min. The size of the polar domains was estimated to be 160 molecules by analyzing the field dependence of the SHG signal intensity on the basis of an Ising model.

DOI: 10.1103/PhysRevE.76.041701

PACS number(s): 61.30.Gd, 61.30.Cz

### I. INTRODUCTION

For materials to be of polar order, the system belongs to symmetry classes of  $C_n$  or  $C_{nv}$ . The dielectrics of its symmetry groups are called pyroelectrics. Particularly, it is called ferroelectrics if the polarization is spontaneously maintained at a zero field and changes its sign upon field reversal. Unless maintained, antiferroelectricity appears in wider symmetry classes with microscopic polar order arranged in an antiparallel manner. Otherwise, the macroscopic polar order is relaxed to randomized microscopic polar-ordered states or helielectric states after removing a field. These antiferroelectricity and randomized polar ordering are distinguishable with and without a threshold of polarization, respectively.

Compared with antiferroelectric polar structures in calamitic [1] and bent-core [2] molecular systems and helielectric polar structures in calamitic [3] and discotic [4,5] molecular systems, less randomized polar structures in liquid crystals are known. One of the recently discovered systems is a randomized polar order in a smectic-*A*-like phase consisting of bent-core molecules [6,7]. In this phase, a few hundreds of molecules form polar order and randomly oriented [8]. This mesoscopic polar-ordered domain easily responds to an electric field to form a uniformly polar-ordered structure [9]. The so-called de Vries smectic-*A* phase [10] provides a similar example when the system is chiral; i.e., a large electroclinic effect in such systems [11] occurs via an electric-field-induced process from randomly tilted molecular assembly to a uniformly tilted smectic- $C^*$  phase. The other intriguing example is switchable columnar phases [12]. Recently, two types of polar columnar liquid crystals were reported: the urea derivative [13] and the polycatenar banana-shaped molecules [14,15]. Both systems have unique intermolecular interactions in a column such as intermolecular hydrogen bonding or packing effect of umbrellalike molecular assemblies. Such soft intermolecular interactions in addition to moderate intercolumnar interactions seem to play an important roll in a reversal of molecular reorientation under an ac field [12]. However, the polar order of these columnar liquid crystals is not held, being conjectured to be randomized polar ordering.

In our previous paper [16], we investigated a polar structure of the hexagonal columnar liquid crystalline phase of *N,N'*-bis(3,4,5-trihexadecyloxyphenyl)urea. The columns consist of linearly linked molecules with hydrogen bonds between urea units. The columns are easily aligned along an applied electric field. Cooperative polarization switching by reversing an applied field was confirmed by means of second-harmonic generation (SHG) interferometry. During such polarization reversal and even after the field removal the column direction is almost preserved. However, the polar order relaxes within about 10 ms after removal of the field [16]. In the course of transient SHG and texture observations, we found that three relaxation processes exist from the field-induced polar structure to the nonpolar ground state over the time range from microseconds to seconds. We report the detailed experimental observations and discuss the relaxation processes from the microscopic (molecular) and macroscopic viewpoints.

### II. EXPERIMENT

The material used in this study was a liquid crystalline urea *N,N'*-bis(3,4,5-trihexadecyloxyphenyl)urea, which showed two columnar phases: hexagonal columnar ( $Col_h$ ) and rectangular columnar ( $Col_r$ ) phases. The phase transition temperatures determined by differential scanning calorimetry was Isotropic (Iso) 164 °C  $Col_h$  137 °C  $Col_r$  on cooling and  $Col_r$  139 °C  $Col_h$  168 °C Iso on heating [13]. Two types of cells were used for texture observation and SHG measurement. For the former cells, one of the glass substrates had a pair of patterned indium-tin-oxide (ITO) electrodes with a gap of 50  $\mu\text{m}$ , so that an in-plane electric field could be applied. For the latter cells, both substrates had square-patterned ITO electrodes to apply a field between the substrates. These substrate surfaces were spin coated with a commercial alignment layer (AL1254, JSR), but not rubbed. These cell thicknesses were controlled by bead spacers and were about 13  $\mu\text{m}$  and 5  $\mu\text{m}$ , respectively. The compound was introduced into these cells in the isotropic phase by cap-

illary suction, and the cells were allowed to cool down to the Col<sub>h</sub> phase (160 °C). The data only at 160 °C will be shown, since the signals at lower temperatures and in the isotropic phase are too weak to analyze the behavior quantitatively.

Two kinds of SHG measurements were made. For the electric field dependence of the SHG intensity, the optical setup for SHG interferometry was used [16]. A quartz plate and a glass plate were inserted between a light source (Nd:YAG laser, Surelite I SLI-10, 10 Hz repetition, 1064 nm wavelength, 6 nm duration, 2 mJ/pulse) and the sample cell with appropriate angles to give the maximum difference between interference fringe extrema under positive and negative field applications. By applying a triangular-wave voltage the interfered SHG signal was detected at elevated triggered positions and sent to a boxcar integrator for accumulation, so that the field dependence of the SHG intensity was obtained. The transient SHG measurements were conducted under the application of bipolar-pulsed electric field as follows. The light source used was a mode-locked Ti:sapphire laser (Vitesse, Coherent), which generated a short pulse train (80 MHz repetition, 800 nm wavelength, 120 fs duration, 280 mW power). The SHG signal detected by photomultiplier tube was integrated by current-to-voltage converter and sent to an oscilloscope (Tektronix) and accumulated. In both measurements, the sample was irradiated at an incidence angle of 45° and *p*-polarized SHG was detected from the transmission direction by the incidence of *p*-polarized fundamental light. Switching current measurements were also conducted by applying the same bipolar-pulsed electric field as that used for the transient SHG measurements at 160 °C.

### III. EXPERIMENTAL RESULTS

Figure 1 shows the temporal variation of the SHG intensity by applying a bipolar-pulsed electric field (dotted line) with different amplitudes between 10 V/μm and 30 V/μm at 160 °C. The overall transient profiles are shown in Fig. 1(a), and the behaviors at the field reversal and the field termination are shown in Figs. 1(b) and 1(c), respectively, in expanded scales. The SHG intensity readily grew just after the field application at  $t=1$  ms and showed a dip right after the field reversal at  $t=3$  ms. Thereafter, the SHG intensity gradually decreased after the field removal at  $t=5$  ms. It is notable that sharp drops in the SHG intensity occur immediately after the field reversal and termination, as indicated by dotted circles in Figs. 1(b) and 1(c). Such rapid SHG changes were observed within a period of 10 μs or less after the reversal or termination of the field, and were followed by slow changes between 100 μs and a few ms, indicating the existence of at least two relaxation processes of the polar structure. We carried out the measurements at different temperatures. The signals became weaker at lower temperatures, so that we could not carry out reliable analysis. However, we confirmed that the overall response became slower with decreasing temperature and the fast component did exist. At the isotropic phase, the signal was weak and the response became faster, so that it was not easy to recognize the existence of the fastest component. Full analysis of the temperature

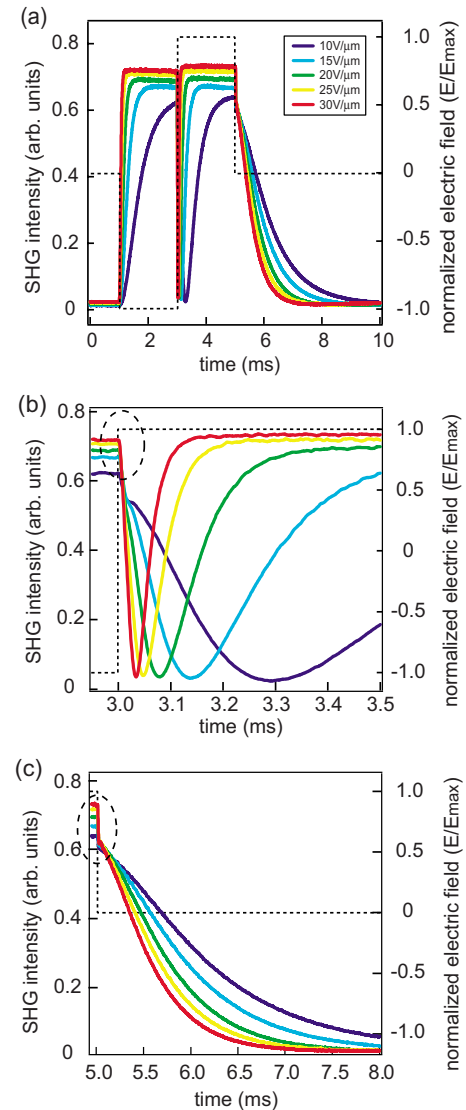


FIG. 1. (Color online) The temporal changes of SHG intensity upon the application of bipolar-pulsed electric field of various amplitudes, whose wave form is shown by a dotted line: (a) overall behavior, (b) behavior upon field reversal in an expanded scale, and (c) behavior upon field termination in an expanded scale. In (b) and (c) sharp drops in the SHG intensity are observed at the first stage, as indicated by dotted circles.

dependence of the transient SHG will be our future work.

To confirm that the transient SHG originates from the polarization switching, switching current measurements were also made using the same condition as that used in the SHG measurement. Figure 2(a) shows the switching current against time under the application of bipolar-pulsed field (dotted line) of various amplitudes. The current behaviors associated with the field reversal and field termination are also shown in Figs. 2(b) and 2(c), respectively.

Let us first examine the fast process in the transient SHG variation. The magnitude of rapid drops in the SHG signal intensity is shown against the applied field in Fig. 3, where solid and open circles correspond to the signals upon reversal and termination of the field. In both cases, the magnitude of

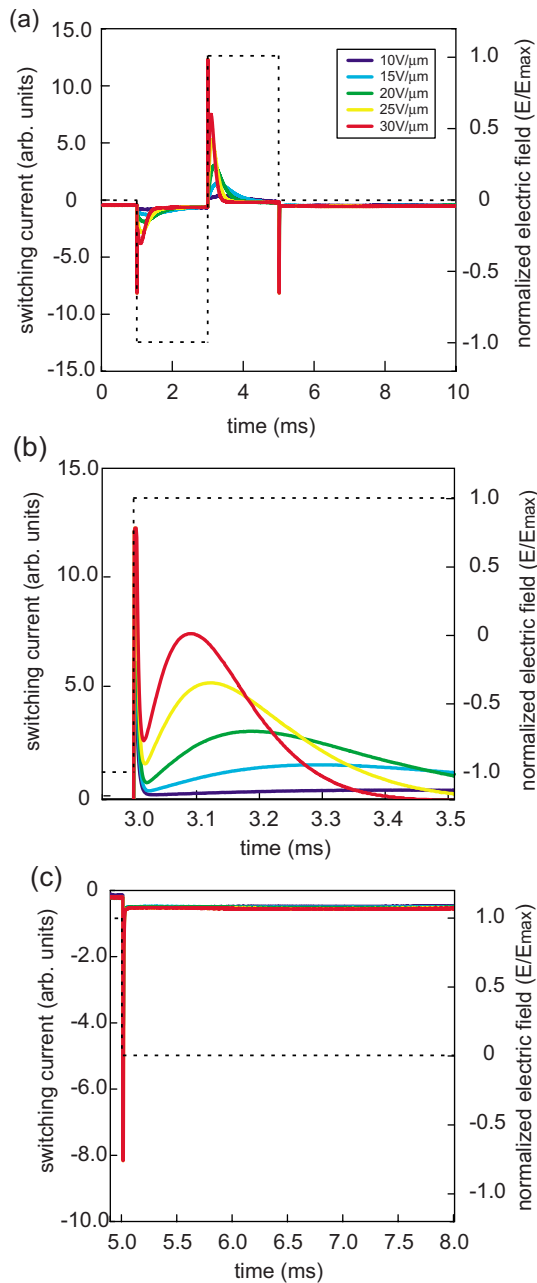


FIG. 2. (Color online) The temporal changes of the switching current upon the application of bipolar-pulsed electric field of various amplitudes: (a) overall behavior, (b) behavior upon field reversal in an expanded scale, and (c) behavior upon field termination in an expanded scale.

the rapid drop increases linearly with the applied field. According to the best fit of the data to linear functions shown by solid lines in Fig. 3, the slope for the field reversal is about twice as large as that for the field termination.

Now we look at the slow process. The rise (fall) time  $\tau$  of the SHG intensity in each process is defined by the time that SHG intensity changes from 10% to 90%—i.e., the SHG variation for the first rise from 0 V to negative fields, the SHG variation between the dip and saturated levels for the field reversal process from negative fields to positive fields, and the SHG variation of the slow process for the field ter-

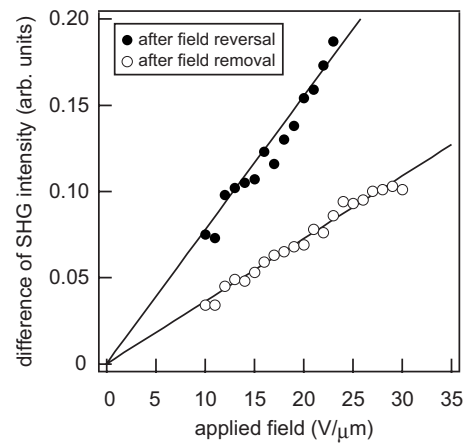


FIG. 3. The SHG intensity drops at the initial stages of field reversal (closed circles) and termination (open circles) as a function of applied field. Note that the gradients of the fitted straight lines are different by a factor of 2.

mination process from positive fields to zero. The data at 10 V/μm were not used for the analysis except for the final relaxation process, since the signal did not saturate. The results are shown in Fig. 4. The data are well fitted to

$$\tau = A/E \tag{1}$$

for the decay process, as shown by a solid curve, and to

$$\tau = B/E^2 \tag{2}$$

for the rise and reversed processes, as shown by dashed curves. Here,  $E$  is the applied field and  $A$  and  $B$  are constants. The following characteristics should be noted. (i) The response time becomes shorter with increasing field strength in all three processes. (ii) The relaxation process is much slower than the polarization-induction processes. (iii) Even

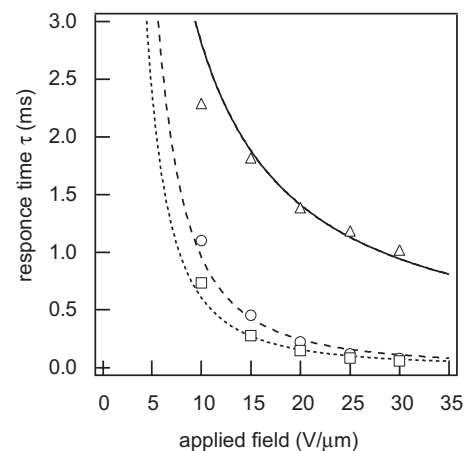


FIG. 4. Response time determined by the SHG intensity change from 10% to 90% as a function of an applied field for three processes of field application (circles), reversal (squares), and termination (triangles). The solid curve is a best fit of the triangles to Eq. (1) and the dashed and dotted curves, respectively, of the circles and the squares to Eq. (2).

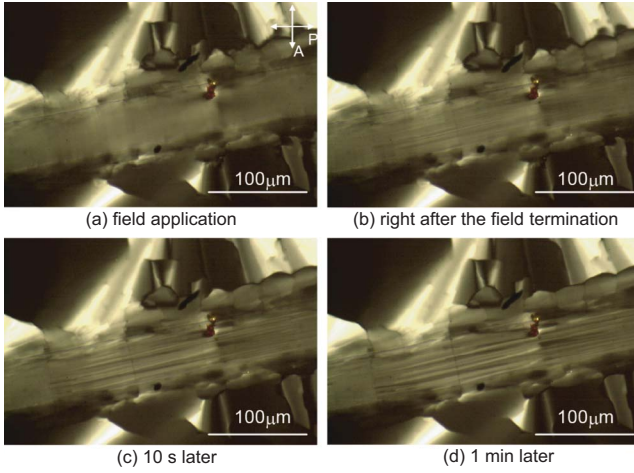


FIG. 5. (Color online) Polarizing optical micrographs (a) during the field application, (b) right after the removal of the field, (c) 10 s later, and (d) 1 min later. Growth of stripe texture becomes obvious at 1 min after the field termination.

in the relaxation process from the same SHG level, the relaxation time is field dependent. Note that the temporal change of the SHG intensity occurred in the same time range as the polarization reversal observed by switching current measurements (Fig. 2). Thus, the SHG variation reflects the polarization switching (see Sec. IV for details).

Next, we show much slower relaxation process observed under a polarizing microscope. Figure 5 shows the continuous change of the texture after removing a triangular wave field of  $6 \text{ V}/\mu\text{m}$  parallel to the substrate surface. In the middle of the micrographs, almost uniformly oriented striped region is seen between electrodes under an electric field. In the uniform bright region shown in Fig. 5(a), the columns were well aligned and the polarization was uniformly oriented between the pair of electrodes. Just after the field removal, narrow stripes perpendicular to the field emerged [Fig. 5(b)]. The width of these stripes grew and became distinct after 10 s [Fig. 5(c)], and finally the structure was stabilized after 1 min [Fig. 5(d)]. Thus the apparent texture change occurs in much longer time scale compared to the relaxation processes observed in the transient SHG measurement.

#### IV. DISCUSSION

Let us first describe the quasistatic polarization switching process. According to the experimental condition, the columns are supposed to be well aligned along the field direction. Cooperative polarization switching is suggested by the SHG activity at low electric fields. Therefore, we can assume that polar molecular assemblies with a polarization  $\mu$  exist and  $\mu$  can take only parallel and antiparallel orientations to the field direction at the initial condition and reorients to the field direction under the field. In the framework of Ising model, we can describe the total polarization  $M$  and the total number of the molecular assemblies  $N$  as

$$M = (N_+ - N_-)\mu, \quad (3)$$

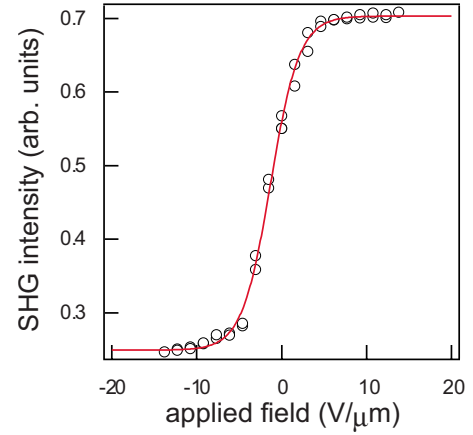


FIG. 6. (Color online) The SHG signal intensity from the sample cell and a quartz plate (reference sample for interference) as a function of an electric field. The best fit to Eq. (7) is shown by a solid curve.

$$N = N_+ + N_-, \quad (4)$$

where  $N_+$  and  $N_-$  are numbers of the assemblies with dipoles  $+\mu$  and  $-\mu$ , respectively. It is well known in the Ising model that the fraction of polarization  $M/N\mu$  is given by

$$\frac{M}{N\mu} = \tanh\left(\frac{\mu E}{kT}\right) \quad (5)$$

under the mean-field approximation. Since the second-order nonlinear susceptibility  $\chi_{\text{eff}}^{(2)}$  is given by

$$\chi_{\text{eff}}^{(2)}(E) = N\mu \tanh\left(\frac{\mu E}{kT}\right), \quad (6)$$

the SHG intensity  $I_{SH}$  observed in the constructive interference condition of the SHG interferometry is given by

$$I_{SH} \propto \left[ N\mu \tanh\left(\frac{\mu E}{kT}\right) + \chi_{\text{quartz}}^{(2)} \right]^2, \quad (7)$$

where  $\chi_{\text{quartz}}^{(2)}$  is the nonlinear susceptibility of quartz used as a reference signal. Figure 6 reveals the SHG intensity obtained in the SHG interferometry by applying a 1-Hz triangular wave field. The fitted curve is the best fit to Eq. (7) with the fitting parameters  $\mu=742 \text{ D}$  and  $T=160 \text{ }^\circ\text{C}$ . Since the dipole moment of urea molecule is about 4.6 D, about 160 molecules form a polar assembly. By taking account of the intermolecular distance along a column 0.48 nm, the length of a polar molecular assembly is at most 77 nm, if the polar domain consists of molecules along a single column. Since this size is much smaller than the wavelength used for the SHG experiments, it is reasonable that no SHG is observed in the absence of an electric field.

We now discuss the relaxation processes. The first question is the cause of the fast process of polarization relaxation in the time range of  $\mu\text{s}$ . One of the possible causes for this fast response is due to the contribution of charge-up and discharge in the capacity constructed by the sample cell, which is not associated with the polarization switching. Actually we always observed the fast current response, as

shown in Fig. 2. To confirm whether the fast response is caused by the capacity contribution or not, we measured transient SHG measurements in other polar liquid crystal systems: (i) switchable columnar phase of polycatenar bent-core molecules [14,15] and (ii) smectic-*A*-like phase of asymmetric bent-core molecules [8,9]. In the former case, we observed the same fast response. In the latter case, however, the major SHG response is so fast that the capacitor contribution cannot be separately detected. Thus, the possible capacity contribution exists.

Another possible contribution to the fast process is due to some relaxation in individual molecules. On the basis of this prerequisite, we consider a model where the molecular hyperpolarizability  $\beta$  changes upon field application. The change of  $\beta$  is possible by the conformational change of molecules; the urea unit in the molecular center is distorted and the wing angle of phenyl groups with respect to the urea unit could be changed by the field application, resulting in the change of intermolecular distance of hydrogen bonding. Upon a negative field application ( $t=1-3$  ms), hyperpolarizability of  $-(\beta+\Delta\beta)$  results, since the hyperpolarizability change  $\Delta\beta$  is induced toward the same direction as the applied field direction. Here  $\Delta\beta$  is assumed to be proportional to the applied field. Upon field reversal, molecules feel the field reversal to positive ( $t=3$  ms), whereas the direction of  $\beta$  does not respond within 10  $\mu$ s, since the reorientation of the polar structure takes a longer time. Hence, the effective hyperpolarizability at the beginning of the field reversal is given by  $-(\beta-\Delta\beta)$ . Thus, the hyperpolarizability changes by  $2\Delta\beta$  at  $t=3$  ms. On the other hand, after sufficiently long application of a positive field ( $t=5$  ms), the molecules possess  $(\beta+\Delta\beta)$ , since the reorientation of the polar order is completed. The hyperpolarizability changes from  $(\beta+\Delta\beta)$  to  $\beta$  at the instance of the field termination, resulting in the hyperpolarizability change of  $\Delta\beta$ .

Since the SHG intensity is proportional to the square of the molecular hyperpolarizability,  $I_{SH}$  is given by

$$I_{SH} \propto \beta^2 + 2\beta \Delta\beta(E) + \Delta\beta(E)^2, \quad (8)$$

when the molecular hyperpolarizability is  $\beta+\Delta\beta$ . Since the induced hyperpolarizability  $\Delta\beta$  is much smaller compare to the intrinsic molecular hyperpolarizability  $\beta$ , the third term of Eq. (8) is neglected. The rapid drop in the SHG intensity in the reverse field process and the decay process  $\Delta I$ 's are, respectively, given by

$$\begin{aligned} \Delta I &= (\beta + \Delta\beta)^2 - (\beta - \Delta\beta)^2 \cong 4\beta \Delta\beta, \\ \Delta I &= (\beta + \Delta\beta)^2 - \beta^2 \cong 2\beta \Delta\beta. \end{aligned} \quad (9)$$

That is why the magnitude of rapid drops in the SHG intensity linearly depends on  $E$ , as shown in Fig. 3. This model also explains the experimental fact that the gradient of the field dependence is larger by a factor of 2 for the field reversal compared with that for the field termination. Since the capacitor contribution mentioned above also has the same features—i.e., linear dependence on  $E$  and the slope difference in Fig. 3 by a factor of 2—we cannot assign the real

cause for the fast component at this moment. This remains as our future problem.

Now we discuss the dynamics occurring in a time range of a few ms. SHG intensity is proportional to the square of the nonlinear polarization, which is different from the induced linear polarization, but must be correlated, and the switching current is given by the time derivative of the induced polarization. Hence, it is natural that the temporal change of the switching current occurs in longer time ranges compared with that of SHG intensity, as observed in Figs. 1 and 2. Therefore, we can conclude that the transient SHG is due to the polarization switching process. It is also noted that the dielectric response occur also in the similar time range; i.e., the relaxation frequency is at about 100 Hz at 160 °C [16]. The polarization switching seems to be driven by the orientation change of the urea units, despite intermolecular hydrogen bonding. For the relaxation process, it is natural to consider that the response time does not depend on the applied field  $E$  at the initial stage (at  $t=5$  ms). Actually, the relaxation time in other systems such as the electroclinic effect [17] and quasipolar smectic-*A*-like phase [9] is constant against the electric field, although the polar-ordered initial states depend on  $E$ . In the present case, the initial state after the fast relaxation is almost the same, being independent of  $E$ , but still the relaxation time  $\tau$  is field dependent given by Eq. (1). It is not easy to find the reason for the field dependence of  $\tau$ . Only the plausible reason is as follows, although the  $E^{-1}$  dependence cannot be explained anyway. It is found in Fig. 1(a) that the saturated SHG intensity slightly depends on the applied field. In other words, the initial condition under different fields has different numbers of defects—i.e., fewer defects under higher field. The subsequent relaxation time  $\tau$  may depend on the defect density at the initial state. In addition, when the field is terminated, fast relaxation occurs, resulting in the same level of SHG. The fast relaxation process was attributed to the relaxation process of individual molecules, as mentioned above. Hence the real initial state is not a stable state but a quasiequilibrium state influenced by the fast relaxation process. In other words, the momentum of inertia of the fast relaxation is possibly transferred to the real initial state. The fact that the decay is not exponential also suggests complicated relaxation mechanisms. Thus, the relaxation time  $\tau$  depends not only on the effective viscosity  $\gamma$  and the effective elastic constant  $K$ , which are included in  $A$  in Eq. (1), but also on the field strength  $E$ .

The field dependence given by Eq. (2) for the rise and reverse processes is now interpreted as follows. Naive consideration leads to the field dependence given by Eq. (1), as well known in the ferroelectric switching in the smectic-*C*\* phase for a uniform molecular rotation process on a cone [18] or for nucleation and growth of polar domains due to the Avrami model [19,20]. Here  $A$  must depend on the effective viscosity  $\gamma$  and the polarization  $\mu$  of a unit polar domain. However, another field-dependent factor mentioned above must be convoluted to the rise and reverse processes. This is why the field dependence is given by Eq. (2).

Finally, we discuss the longest relaxation process, as observed by optical micrographs in Fig. 5. The development of a stripe texture suggests the undulation structure of columns, as illustrated in Fig. 7. After the field is removed, the mac-

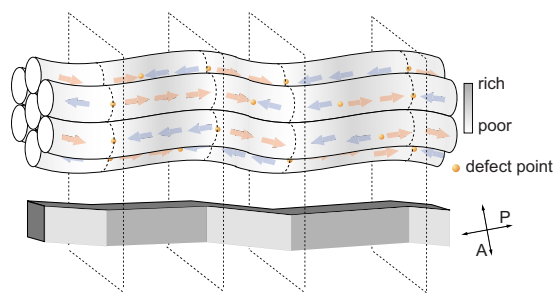


FIG. 7. (Color online) The model of column undulation structure. Microscopic polar domains are illustrated by arrows, and the slightly hatched portion stands for higher molecular density. Birefringence colors resulted from the column orientation are illustrated at the bottom.

roscopic polar structure cannot be preserved and half of the polar domains must be reversed to escape from the macroscopic polarization. Since uniform head-to-tail orientation of dipole is the most stable orientation from the viewpoint of dipole-dipole interaction, this orientation seems to give a straight column with higher molecular density. On the contrary, the molecular density at the defect position becomes less dense and easy to bend because of the repulsion of microscopic polar orders. Since the defect points can easily move in a column by local molecular flip-flop reorientation (soliton movement), the defects tend to gather in the vicinity of the bend portion of columns. Consequently the structure shown in Fig. 7 is formed. In the figure, higher density portion of molecules are slightly hatched. Of course, it is natural

to imagine that not all the defect points gather to the bent portion by considering the number of molecules included in each polar domain. X-ray results support this model: A broad halo attributed to the intermolecular distance in a column indicates the broad dispersion of the distance between intermolecular hydrogen bonds. Similar textures were observed in smectics and banana-shaped mesogens [21] and the similar origin as the density fluctuation was considered.

## V. CONCLUSIONS

We observed three relaxation processes from a field-induced polar structure in a columnar liquid crystalline urea derivative by means of SHG and polarizing optical microscopy. SHG indicates two processes: fastest and intermediate. The fastest process of about  $10 \mu\text{s}$  or less originates from either the capacity contribution or the relaxation of molecular level. The intermediate speed process observed between  $100 \mu\text{s}$  and a few ms is due to the polarization switching of polar domains: the molecular assembly level. The slowest process was observed by optical microscopy. The relaxation occurs within 1 min and is attributed to the change in column assembly level. The size of the polar domain was also estimated to be 160 molecules by applying an Ising model to the field dependence of the SHG signal intensity.

## ACKNOWLEDGMENT

This work is partly supported by Grant-in-Aid for Scientific Research (S) (No. 16105003) from the Ministry of Education, Culture, Science, Sports and Technology of Japan.

- 
- [1] A. D. L. Chandani, E. Gorecka, Y. Ouchi, H. Takezoe, and A. Fukuda, *Jpn. J. Appl. Phys., Part 2* **28**, L1265 (1989).
- [2] H. Takezoe and Y. Takanishi, *Jpn. J. Appl. Phys., Part 1* **45**, 597 (2006).
- [3] R. B. Meyer, L. Liebert, L. Strzelecki, and P. Keller, *J. Phys. (Paris)* **36**, L69 (1975).
- [4] G. Scherowsky and X. H. Chen, *Liq. Cryst.* **17**, 803 (1994).
- [5] H. Bock and W. Helfrich, *Liq. Cryst.* **18**, 707 (1995).
- [6] D. Pociecha, E. Gorecka, M. Čepič, N. Vaupotič, and W. Weissflog, *Phys. Rev. E* **74**, 021702 (2006).
- [7] D. Pociecha, E. Gorecka, M. Čepič, N. Vaupotič, K. Gomola, and J. Mieczkowski, *Phys. Rev. E* **72**, 060701(R) (2005).
- [8] Y. Shimbo, E. Gorecka, D. Pociecha, F. Araoka, M. Goto, Y. Takanishi, K. Ishikawa, J. Mieczkowski, K. Gomola, and H. Takezoe, *Phys. Rev. Lett.* **97**, 113901 (2006).
- [9] Y. Shimbo, Y. Takanishi, K. Ishikawa, E. Gorecka, D. Pociecha, J. Mieczkowski, K. Gomola, and H. Takezoe, *Jpn. J. Appl. Phys., Part 2* **45**, L282 (2006).
- [10] A. J. de Vries, *Mol. Cryst. Liq. Cryst.* **41**, 27 (1977).
- [11] N. A. Clark, T. Bellini, R.-F. Shao, D. Coleman, S. Bardon, D. R. Link, J. E. MacLennan, X.-H. Chen, M. D. Wand, D. M. Walba, P. Rudquist, and S. T. Lagerwall, *Appl. Phys. Lett.* **80**, 4097 (2002).
- [12] H. Takezoe, K. Kishikawa, and E. Gorecka, *J. Mater. Chem.* **16**, 2412 (2006).
- [13] K. Kishikawa, S. Nakahara, Y. Nishikawa, S. Kohmoto, and M. Yamamoto, *J. Am. Chem. Soc.* **127**, 2565 (2005).
- [14] E. Gorecka, D. Pociecha, J. Mieczkowski, J. Matraszek, D. Guillon, and B. Donnio, *J. Am. Chem. Soc.* **126**, 15946 (2004).
- [15] E. Gorecka, D. Pociecha, J. Matraszek, J. Mieczkowski, Y. Shimbo, Y. Takanishi, and H. Takezoe, *Phys. Rev. E* **73**, 031704 (2006).
- [16] Y. Okada, S. Matsumoto, Y. Takanishi, K. Ishikawa, S. Nakahara, K. Kishikawa, and H. Takezoe, *Phys. Rev. E* **72**, 020701(R) (2005).
- [17] A. D. L. Chandani, Y. Ouchi, H. Takezoe, and A. Fukuda, in *Dynamic Behavior of Macromolecules, Colloids, Liquid Crystals and Biological Systems*, edited by H. Watanabe (Hirokawa, Tokyo, 1989), p. 399.
- [18] M. A. Handschy and N. A. Clark, *Opt. Eng. (Bellingham)* **23**, 261 (1984).
- [19] H. Orihara and Y. Ishibashi, *Jpn. J. Appl. Phys., Part 1* **23**, 1274 (1984).
- [20] M. Avrami, *J. Chem. Phys.* **9**, 177 (1941).
- [21] D. A. Coleman, J. Fernsler, N. Chattham, M. Nakata, Y. Takanishi, E. Korblova, D. R. Link, R.-F. Shao, W. G. Jang, J. E. MacLennan, O. Mondainn-Monval, C. Boyer, W. Weissflog, G. Pelzl, L.-C. Chien, J. Zasadzinski, J. Watanabe, D. M. Walba, H. Takezoe, and N. A. Clark, *Science* **301**, 1204 (2003).